

# POLARIZED INFRARED EMISSION BY POLYCYCLIC AROMATIC HYDROCARBONS RESULTING FROM ANISOTROPIC ILLUMINATION

LORENZO SIRONI AND BRUCE T. DRAINE

Princeton University Observatory, Peyton Hall, Princeton, NJ 08544-1001

*Draft version June 5, 2022*

## ABSTRACT

We study the polarized infrared emission by Polycyclic Aromatic Hydrocarbons (PAHs), when anisotropically illuminated by UV photons. PAH molecules are modeled as planar disks with in-plane and out-of-plane vibrational dipoles. As first pointed out by Leger (1988), infrared emission features resulting from in-plane and out-of-plane modes should have orthogonal polarization directions. We show analytically how the degree of polarization depends on the viewing geometry and the molecule's internal alignment between principal axis of inertia and angular momentum, which gets worse after photon absorption. Longer wavelength features, emitted after better internal alignment is recovered, should be more strongly polarized. The degree of polarization for uni-directional illumination (e.g., by a star) is larger than for diffuse illumination (e.g., by a disk galaxy), all else being equal. For PAHs in the Cold Neutral Medium, the predicted polarization is probably too small to distinguish from the contribution of linear dichroism by aligned foreground dust. The level of polarization predicted for PAH emission from the Orion Bar is only  $\approx 0.06\%$  at  $3.3\ \mu\text{m}$ ; Sellgren et al. (1988) report a much larger value,  $0.86 \pm 0.28\%$ , which suggests that the smallest PAHs may have moderately suprathermal rotation rates. Future observations of (or upper limits on) the degree of polarization for the Orion Bar or for dust above edge-on galaxies (e.g., NGC 891 or M82) may constrain the internal alignment of emitting PAHs, thus providing clues to their rotational dynamics.

*Subject headings:* ISM: dust, extinction — ISM: general — infrared: galaxies

## 1. INTRODUCTION

The strong infrared emission features at  $3.3$ ,  $6.2$ ,  $7.7$ ,  $8.6$ ,  $11.3$  and  $12.7\ \mu\text{m}$  have been attributed to vibrational modes in planar Polycyclic Aromatic Hydrocarbons (PAHs) (e.g., Leger & Puget 1984; Allamandola et al. 1985). Additional strong features at  $16.4$  and  $\sim 17\ \mu\text{m}$  (e.g., Smith et al. 2007) have also been attributed to PAHs, although the identification is less certain. Leger (1988) noted that a planar PAH molecule may emit partially polarized light if anisotropically illuminated by a source of UV photons. The basic reasons are the following: *i*) UV absorption is favored if the molecule faces the illuminating source; *ii*) spinning of the molecule around its angular momentum preserves some memory of the illumination direction; *iii*) the vibrational dipoles responsible for the IR emission features oscillate either perpendicular or parallel to the molecular plane. In particular, the C-H stretching mode ( $3.3\ \mu\text{m}$ ) and the in-plane C-H bending mode ( $8.6\ \mu\text{m}$ ) oscillate parallel to the grain plane, whereas the out-of-plane C-H bending mode ( $11.3$  and  $12.7\ \mu\text{m}$ ) oscillates perpendicular to the molecular plane. The strong emission features at  $6.2$  and  $7.7\ \mu\text{m}$  are believed to arise from in-plane C-C stretching and bending modes. In-plane modes ( $3.3$ ,  $6.2$ ,  $7.7$ ,  $8.6\ \mu\text{m}$ ) and out-of-plane modes ( $11.3$ ,  $12.7\ \mu\text{m}$ ) should exhibit orthogonal polarization angles (Leger 1988), and their electric field vector should be respectively perpendicular and parallel to the plane-of-sky projection of the illumination direction.

Sellgren et al. (1988) have searched for linear polarization of the  $3.3$  and  $11.3\ \mu\text{m}$  emission features in a variety

of astronomical sources where PAH emission is observed offset from the illuminating source. Their upper limits on the degree of polarization are of the order a few percent. At one position on the Orion Bar they measure a linear polarization of  $0.86 \pm 0.28\%$  in the  $3.3\ \mu\text{m}$  feature, with the polarization angle consistent with being orthogonal to the line between the nebula and the star, as predicted by Leger (1988). However, as we show below, the polarization they report for the  $3.3\ \mu\text{m}$  feature is much larger than expected.

In this work we present analytic formulae for the degree of polarization of the PAH emission features, when the emitting grains are anisotropically illuminated. We model PAH molecules as planar disks with in-plane and out-of-plane vibrational dipoles. We extend the calculations by Leger (1988) to allow for an arbitrary degree of disalignment between the molecule's principal axis of inertia  $\hat{\mathbf{a}}_1$  (perpendicular to the molecular plane) and its angular momentum  $\mathbf{J}$ . We discuss both the case of a point-like illuminating source, which may be applied to reflection nebulae like the Orion Bar, and of an extended source (e.g., a disk galaxy), which may be relevant for dust above NGC 891 or M82. The level of polarization is sensitive to the angle between the line of sight and the illumination direction, and to the degree of alignment between  $\hat{\mathbf{a}}_1$  and  $\mathbf{J}$ . Measurements of the degree of polarization can therefore provide insight into the rotational dynamics of PAHs.

This work is organized as follows: in §2 we describe our model for UV absorption and polarized IR emission by PAH molecules, commenting on uncertainties regarding the alignment of  $\hat{\mathbf{a}}_1$  with  $\mathbf{J}$ ; in §3 we present our results, both for a star-like illuminating source and for an extended galactic disk. The reader interested primarily in

the observational implications of our work may wish to skip §2 and §3 and proceed directly to §4, where we summarize our findings and discuss how future polarization measurements may constrain the geometrical and rotational properties of PAHs.

## 2. MODEL FOR POLARIZED EMISSION FROM PAHs

As discussed by Leger (1988), planar PAH molecules may emit partially polarized light as a result of anisotropic illumination by a source of UV photons. UV absorption is favored if the molecular plane is perpendicular to the illumination direction. Following UV absorption, in-plane and out-of-plane vibrational modes are excited, producing the observed IR emission features.

The grain angular momentum  $\mathbf{J}$  stays approximately constant during the whole process of UV absorption and IR emission (Leger 1988): first, the angular momentum contributed by the absorbed UV photon or removed via vibrational IR emission or rotational radio emission is small compared to the mean angular momentum of interstellar PAHs; secondly, collisions of the emitting grain with interstellar atoms or ions hardly occur during the few seconds of IR emission; finally, Larmor precession of  $\mathbf{J}$  around the interstellar magnetic field takes much longer than the IR emission burst (Rouan et al. 1992). With  $\mathbf{J}$  conserved, some memory of the source direction is retained and the IR emission bands will be partially polarized.

### 2.1. Illumination geometry

We adopt the system of coordinates used by Leger (1988) to specify the illumination geometry and the orientation of the emitting molecule (Fig. 1). The fixed coordinate system  $(\hat{x}, \hat{y}, \hat{z})$  is centered on the emitting grain; the polar axis  $\hat{z}$  is along the illumination direction and  $\hat{x}$  is in the plane defined by  $\hat{z}$  and the direction  $\hat{n}$  from the molecule to the observer (Fig. 1 *a*). In this frame, the grain angular momentum  $\mathbf{J}$  has spherical angles  $\theta$  and  $\varphi$  (Fig. 1 *b*). In order to describe the position of the molecule with respect to  $\mathbf{J}$ , we define a frame  $(\hat{x}', \hat{y}', \hat{z}')$  centered on the grain with  $\hat{z}'$  along  $\mathbf{J}$  and  $\hat{x}'$  perpendicular to the plane  $(\hat{z}, \hat{z}')$ , as shown in Fig. 1 *b*. We choose the grain axes of inertia  $(\hat{a}_1, \hat{a}_2, \hat{a}_3)$  so that  $\hat{a}_1$  is the axis of largest moment of inertia (i.e., the principal axis); for a disk molecule,  $\hat{a}_1$  is perpendicular to the plane of the molecule, whereas  $\hat{a}_2$  and  $\hat{a}_3$  are in the plane. Their position in the frame  $(\hat{x}', \hat{y}', \hat{z}')$  is described with Euler's angles (Fig. 1 *c*):  $\beta$ , nutation angle, between  $\hat{z}'$  (or  $\mathbf{J}$ ) and  $\hat{a}_1$ ;  $\psi$ , precession angle, between  $\hat{x}'$  and the line of nodes, i.e., the intersection of the plane  $(\hat{x}', \hat{y}')$  with the molecular plane  $(\hat{a}_2, \hat{a}_3)$ ;  $\phi$ , angle of proper rotation, between the line of nodes and  $\hat{a}_2$ . The classical motion of a rigid axisymmetric grain is a combined rotation around its symmetry axis  $\hat{a}_1$  and a precession of this axis around the angular momentum  $\mathbf{J}$  with constant  $\beta$ .<sup>1</sup> To describe the polarization of the emitted radiation, we define  $\alpha$ , the angle between the illumination direction  $\hat{z}$  and the observer direction  $\hat{n}$ , and the polarization directions  $\hat{u}$  and  $\hat{v}$ , respectively parallel and perpendicular to  $\hat{y}$  in the plane of the sky (Fig. 1 *a*).

<sup>1</sup> For a perfectly symmetric grain, the moments of inertia  $I_2$  and  $I_3$  corresponding to  $\hat{a}_2$  and  $\hat{a}_3$  are equal and no nutation occurs.

### 2.2. Cross section for absorption of starlight

The absorption cross section for incident light with electric field  $\mathbf{E}$  is proportional to (Leger 1988)

$$A \propto \sum_{i,j} |\langle j | \mathbf{E} \cdot \mathbf{d} | i \rangle|^2, \quad (1)$$

where the summation is over molecular states  $|i\rangle$  and  $|j\rangle$  and  $\mathbf{d}$  is the electric dipole moment operator. The  $\pi - \pi^*$  electronic transitions responsible for UV absorption in PAHs have  $\langle j | \mathbf{d} | i \rangle$  only in the molecular plane. For a disk molecule, rapid spinning around its principal axis  $\hat{a}_1$  results in averaging over the angle of proper rotation  $\phi$ . Thus, the grain absorption cross section may be written, for incident unpolarized light,

$$A \propto (1 + \cos^2 \Theta) \quad (2)$$

where  $\Theta$  is the angle between the normal to the grain plane (i.e., the principal axis  $\hat{a}_1$ , for a disk molecule) and the direction of propagation  $\hat{\mathbf{k}}$  of the absorbed photon. In other words, when a planar PAH faces an unpolarized source, its UV absorption cross section is twice that when it is edge-on, because both components of the illuminating electric field can be absorbed in the first case and only one in the second.

The angle  $\Theta$  depends on the instantaneous orientation of the grain with respect to the illumination direction. However, since the precession period of  $\hat{a}_1$  around  $\mathbf{J}$  is much shorter than the time between absorption and emission, we can average over the precession motion (and the precession angle  $\psi$ ) for the absorption and the emission process independently. For a point-like illuminating source, all incoming rays have  $\hat{\mathbf{k}} = \hat{z}$  (see Fig. 1 *a*). The corresponding  $\psi$ -averaged absorption cross section, for fixed  $\mathbf{J}$  and a fixed angle  $\beta$  between  $\hat{a}_1$  and  $\mathbf{J}$ , is

$$\begin{aligned} \bar{A}_*(\theta, \beta) &= 1 + \cos^2 \theta \cos^2 \beta + \frac{1}{2} \sin^2 \theta \sin^2 \beta \\ &\equiv 1 + C(\theta, \beta) \quad . \end{aligned} \quad (3)$$

If the illuminating source is an extended disk galaxy, the angle  $\Theta$  also depends on the spherical angles  $\theta'$  and  $\varphi'$  of the ray direction  $\hat{\mathbf{k}}$  in the fixed  $(\hat{x}, \hat{y}, \hat{z})$  frame. We assume that the emitting molecules are above the galactic center;  $\hat{z}$  is then the direction from the center of the galactic disk to the grains. For an axisymmetric surface-brightness profile, the absorption coefficient for incoming rays with polar angle  $\theta'$  can be averaged over the azimuthal illumination angle  $\varphi'$ :

$$\bar{A}_{\text{gal}}(\theta, \beta, \theta') = 1 + \cos^2 \theta' C(\theta, \beta) + \sin^2 \theta' S(\theta, \beta) \quad , \quad (4)$$

where we have also averaged over the precession angle  $\psi$ . In the previous expression,  $C(\theta, \beta)$  is the same as in eq. (3) and we define

$$S(\theta, \beta) \equiv \frac{1}{4} (1 + \cos^2 \theta) \sin^2 \beta + \frac{1}{2} \sin^2 \theta \cos^2 \beta \quad . \quad (5)$$

For the sake of simplicity, in the following we assume a uniform-brightness disk galaxy; for a generic axisymmetric brightness profile  $B(\theta')$ , the absorption cross section in eq. (4) should be convolved with  $B(\theta')$ . As a special case, we observe that if  $\theta' = 0$  for all incoming rays, i.e.

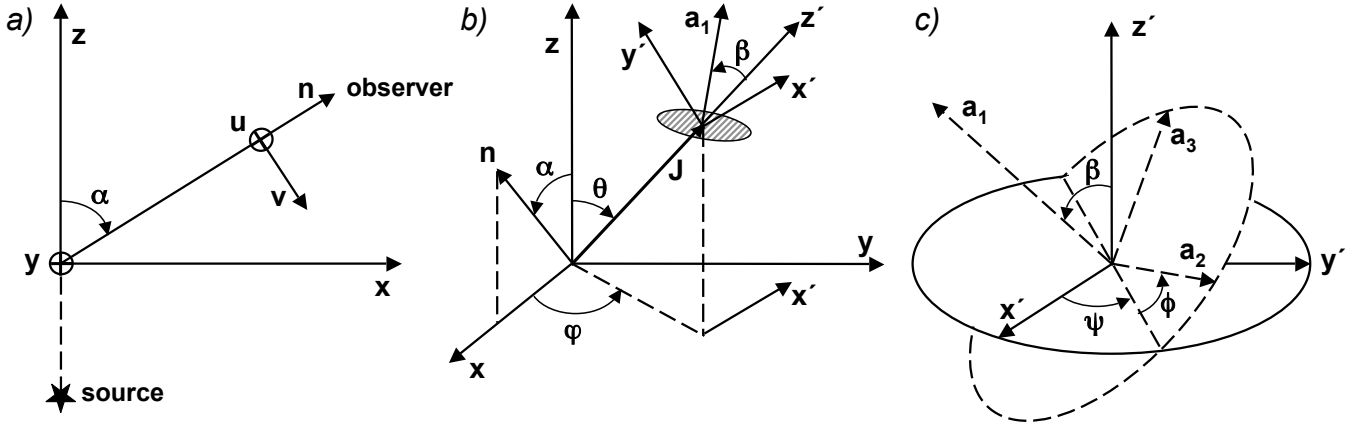


FIG. 1.— Geometry of the star-molecule-observer system, as presented by Leger (1988). In *b*), the molecule (dashed disk) has been moved far from the center of  $(\hat{x}, \hat{y}, \hat{z})$  for clarity. See §2.1 for details.

$\hat{\mathbf{k}} = \hat{\mathbf{z}}$ , we recover the absorption cross section in eq. (3) for a point-like illuminating source.

### 2.3. Cross section for polarized emission

The cross section for PAH emission polarized along a direction  $\hat{\mathbf{w}}$  is proportional to (Leger 1988)

$$F_w \propto \sum_{j,k} |\langle k | \hat{\mathbf{w}} \cdot \mathbf{d} | j \rangle|^2, \quad (6)$$

where  $|j\rangle$  and  $|k\rangle$  are vibrational states of the emitting molecule. We shall call  $F_w^{\parallel}$  and  $F_w^{\perp}$  the relative emission cross sections for in-plane and out-of-plane modes respectively. For out-of-plane modes, the only non-vanishing terms in eq. (6) involve the component of  $\mathbf{d}$  perpendicular to the molecule plane, and

$$F_w^{\perp} = (\hat{\mathbf{a}}_1 \cdot \hat{\mathbf{w}})^2. \quad (7)$$

For in-plane modes, the matrix elements in eq. (6) are non-zero only for the components of  $\mathbf{d}$  in the molecule plane; for a rapidly-spinning disk molecule, rotational invariance with respect to the angle of proper rotation  $\phi$  yields

$$F_w^{\parallel} = 1 - (\hat{\mathbf{a}}_1 \cdot \hat{\mathbf{w}})^2 = 1 - F_w^{\perp}. \quad (8)$$

By averaging over the precession angle  $\psi$  for the emission process independently from the absorption (as discussed in §2.2), the emission cross sections for out-of-plane modes with polarization along  $\hat{\mathbf{u}}$  and  $\hat{\mathbf{v}}$  are

$$\begin{aligned} \bar{F}_u^{\perp}(\theta, \varphi, \beta, \alpha) &= \frac{1}{2}(\cos^2 \varphi + \cos^2 \theta \sin^2 \varphi) \sin^2 \beta \\ &+ \sin^2 \theta \sin^2 \varphi \cos^2 \beta, \end{aligned} \quad (9)$$

$$\begin{aligned} \bar{F}_v^{\perp}(\theta, \varphi, \beta, \alpha) &= \cos^2 \alpha \left[ \frac{1}{2}(\sin^2 \varphi + \cos^2 \theta \cos^2 \varphi) \sin^2 \beta \right] \\ &+ \cos^2 \alpha \sin^2 \theta \cos^2 \varphi \cos^2 \beta + \sin^2 \alpha C(\theta, \beta) \\ &+ \frac{1}{4} \sin 2\alpha \sin 2\theta \cos \varphi (1 - 3 \cos^2 \beta), \end{aligned} \quad (10)$$

where  $C(\theta, \beta)$  has been defined in eq. (3). We have made use of the fact that the orientation of the angular momentum  $\mathbf{J}$  is constant during the IR emission burst, as discussed at the beginning of §2.

The corresponding emission cross sections for in-plane modes with polarization along  $\hat{\mathbf{u}}$  and  $\hat{\mathbf{v}}$  can be computed from their out-of-plane counterparts by using eq. (8):

$$\bar{F}_u^{\parallel}(\theta, \varphi, \beta, \alpha) = 1 - \bar{F}_u^{\perp}(\theta, \varphi, \beta, \alpha), \quad (11)$$

$$\bar{F}_v^{\parallel}(\theta, \varphi, \beta, \alpha) = 1 - \bar{F}_v^{\perp}(\theta, \varphi, \beta, \alpha). \quad (12)$$

By averaging over the azimuthal angle  $\varphi$  of the angular momentum distribution, we simplify eqs. (9)-(10) and obtain

$$\bar{F}_u^{\perp}(\theta, \beta, \alpha) = S(\theta, \beta), \quad (13)$$

$$\bar{F}_v^{\perp}(\theta, \beta, \alpha) = \cos^2 \alpha S(\theta, \beta) + \sin^2 \alpha C(\theta, \beta), \quad (14)$$

and the corresponding  $\varphi$ -averaged cross sections for in-plane modes may then be derived from eq. (8). In the following, we assume that the angular momentum  $\mathbf{J}$  is randomly oriented in space, but in principle eqs. (9)-(10) and eqs. (11)-(12) could be convolved with any angular distribution for  $\mathbf{J}$ , e.g., if the emitting molecules are partially aligned by the interstellar magnetic field.

### 2.4. Model for the alignment of $\hat{\mathbf{a}}_1$ with $\mathbf{J}$

The probability that a symmetric grain rotates with angular momentum  $J \equiv |\mathbf{J}|$  and nutation angle  $\beta$  (between  $\hat{\mathbf{a}}_1$  and  $\mathbf{J}$ ) may be written (e.g., Lazarian & Draine 1997)

$$dP(J, \beta) \propto f(J) \exp\left(-\frac{E_{\text{rot}}(J, \beta)}{k_B T_{\text{ia}}}\right) \sin \beta d\beta dJ, \quad (15)$$

where  $f(J)dJ$  is the probability that the angular momentum  $\in [J, J+dJ]$ ,  $E_{\text{rot}}$  is the grain rotational energy and  $T_{\text{ia}}$  is the ‘‘internal alignment’’ temperature which parametrizes the degree of alignment between  $\hat{\mathbf{a}}_1$  and  $\mathbf{J}$ . In the classical approximation, the rotational energy of a symmetric oblate grain is

$$E_{\text{rot}}(J, \beta) = \frac{J^2}{2I_1} \left[ 1 + \left( \frac{I_1}{I_2} - 1 \right) \sin^2 \beta \right], \quad (16)$$

where  $I_1$  is the largest moment of inertia, corresponding to  $\hat{\mathbf{a}}_1$ , and  $I_2 = I_3 < I_1$ ; for a planar symmetric molecule,  $I_2 = I_3 = I_1/2$ . For the sake of simplicity, we assume that all the emitting molecules have the same moments of inertia.

The absorption (eqs. (3)-(4)) and emission (eqs. (9)-(12)) cross sections do not depend on  $J$  but only on the angle  $\beta$  between  $\hat{\mathbf{a}}_1$  and  $\mathbf{J}$ . Therefore, we may integrate eq. (15) with respect to  $J$ , provided  $f(J)$  is known, and the resulting probability distribution will be used to describe the degree of alignment between  $\hat{\mathbf{a}}_1$  and  $\mathbf{J}$  when we compute the PAH polarized emission in §3. In the simple case  $f(J) \propto \delta(J - \bar{J})$  (or, in general, if  $f(J)$  is strongly peaked at  $\bar{J}$ ), the probability distribution in eq. (15) reduces to

$$dP_\gamma(\beta) = \frac{\sqrt{\gamma} \exp(-\gamma \sin^2 \beta) \sin \beta d\beta}{\sqrt{\pi} e^{-\gamma} \operatorname{erfi}(\sqrt{\gamma})}, \quad (17)$$

where  $\operatorname{erfi}(z) \equiv (2/\sqrt{\pi}) \int_0^z \exp(t^2) dt$  is the imaginary error function. We have defined a dimensionless “internal alignment” coefficient

$$\gamma \equiv \frac{\bar{J}^2}{2I_1 k_B T_{\text{ia}}} \left( \frac{I_1}{I_2} - 1 \right) \equiv \frac{T_{\text{rot}}}{T_{\text{ia}}} \left( \frac{I_1}{I_2} - 1 \right), \quad (18)$$

where  $T_{\text{rot}} \equiv \bar{J}^2/2I_1 k_B$ . When  $\gamma \rightarrow \infty$ , the molecule principal axis tends to be perfectly aligned with the angular momentum; when  $\gamma = 0$ ,  $\hat{\mathbf{a}}_1$  is randomly oriented with respect to  $\mathbf{J}$ .

As discussed at the beginning of §2,  $\mathbf{J}$  stays approximately constant between UV absorption and IR emission, and so does  $T_{\text{rot}}$ ; however, the molecule internal alignment temperature  $T_{\text{ia}}$  may substantially change if part of the absorbed photon energy is transferred to rotational degrees of freedom. We account for the uncertain energy exchange between vibrational and rotational modes by parametrizing the grain internal alignment before UV absorption and during IR emission respectively with  $\gamma_0$  (corresponding to  $T_{\text{ia}} \equiv T_0$ ) and  $\gamma_r \leq \gamma_0$  (corresponding to  $T_{\text{ia}} \geq T_0$ ). In principle,  $\gamma_r$  should be different for each IR emission feature, since it may be thought of as the internal alignment coefficient when most of the radiation in that band is emitted.

We now discuss another plausible choice for the parametrization of the alignment between  $\hat{\mathbf{a}}_1$  and  $\mathbf{J}$  prior to UV absorption. If many collisions with hydrogen atoms occur in the interval between two UV absorptions, and there are no other torques acting, the grain will be driven towards “Brownian rotation” with  $f(J) \propto J^2$ . If there is no vibrational-rotational energy exchange (i.e., the PAH acts like a rigid rotator), the internal alignment temperature  $T_0$  before UV absorption will approximately equal the gas kinetic temperature  $T_{\text{gas}}$ . Integration of eq. (15) with respect to  $J$  assuming  $f(J) \propto J^2$  yields a probability distribution

$$dP_\epsilon(\beta) = \frac{\epsilon(\epsilon - 1)^{1/2} \sin \beta d\beta}{2(\epsilon - \cos^2 \beta)^{3/2}}, \quad (19)$$

which does not depend on  $T_{\text{gas}}$  but only on the geometrical properties of the grain via  $\epsilon \equiv I_1/(I_1 - I_2)$ .

In the following, we parametrize the disalignment between  $\hat{\mathbf{a}}_1$  and  $\mathbf{J}$  by using eq. (17) both before UV absorption (with  $\gamma_0$ ) and during IR emission (with  $\gamma_r \leq \gamma_0$ ). However, in the Appendix we present analytic formulae for the expected degree of polarization if the grain alignment before UV absorption can be described by eq. (19), but eq. (17) still holds during IR emission.

## 2.5. Estimating $\gamma_0$ and $\gamma_r$

In the dust model of Draine & Li (2007), the 3 – 13  $\mu\text{m}$  emission features are produced primarily by PAH molecules or clusters containing between  $N_C \approx 25$  and  $\sim 1000$  carbon atoms, and the 17  $\mu\text{m}$  complex is mainly due to PAHs with  $N_C \approx 2000$ . For purposes of estimating rotational kinetic energies and the density of vibrational states, we will take  $N_C = 200$  as a representative value, with a volume-equivalent radius  $a \approx 7.5 \text{ \AA}$ . We suppose that all the emitting molecules are axisymmetric and planar, with  $I_1/I_2 = 2$ .

Following UV absorption, the alignment between the molecule principal axis  $\hat{\mathbf{a}}_1$  and angular momentum  $\mathbf{J}$ , and thus the internal alignment temperature  $T_{\text{ia}}$ , depends on the efficacy of internal energy exchange between lattice vibrational modes and rotational modes. The Intramolecular Vibration-Rotation Energy Transfer (IVRET) process (Purcell 1979), due to imperfect elasticity of the molecule when stressed by centrifugal and Coriolis forces, allows energy exchange between rotation and vibrations on a timescale  $\sim 10^{-2}$  s (Rouan et al. 1992), much shorter than the duration  $\sim 1 - 10$  s of the IR emission burst. This means that, while the molecule is cooling after UV absorption, its internal alignment temperature  $T_{\text{ia}}$  tends to be equal to the instantaneous vibrational (lattice) temperature  $T_{\text{vib}}$ . Following photon absorption, the lattice may be heated up to a temperature  $T_{\text{vib}} \approx 300 - 1500$  K, depending on the grain size and the photon energy. The grain cools as IR energy is radiated, and we estimate  $T_{\text{vib}} \approx 800$  K when most of the 3.3  $\mu\text{m}$  emission takes place,  $T_{\text{vib}} \approx 300$  K for the 7.7  $\mu\text{m}$  emission,  $T_{\text{vib}} \approx 200$  K for the 11.3  $\mu\text{m}$  emission, and  $T_{\text{vib}} \approx 120$  K for the 17  $\mu\text{m}$  emission, unless the local radiation field is so intense to prevent the lattice from cooling down to such temperatures.

The internal temperature  $T_{\text{ia}}$  follows  $T_{\text{vib}}$  while the grain is cooling, with  $T_{\text{ia}} \approx T_{\text{vib}}$  as long as the vibrational energy levels are sufficiently closely spaced to allow energy transfer between vibrations and rotation.<sup>2</sup> When the separation  $\Delta E$  of vibrational levels exceeds  $\sim \hbar\omega_{\text{rot}}$ , the IVRET process ceases to operate and the rotational modes decouple from the lattice. The density of states can be calculated using a model normal mode spectrum and the Beyer-Swinehart algorithm (Draine & Li 2001): for  $N_C = 200$ , the density of states at vibrational energy  $E/hc \approx 250 \text{ cm}^{-1}$  is  $hc dN/dE \approx 1/(0.18 \text{ cm}^{-1})$ . This should still allow energy exchange in quanta  $\Delta E/hc \sim (\omega_{\text{rot}}/2\pi c) \approx 0.33 \text{ cm}^{-1}$  for a grain spinning at  $\omega_{\text{rot}}/2\pi \approx 10$  GHz, so that the rotational and vibrational modes will decouple only when the lattice vibrational energy has dropped below  $E/hc \approx 250 \text{ cm}^{-1}$ . For our model PAH, this is the average energy if it were in contact with a  $\sim 65$  K heat bath, which suggests  $T_0 \approx 65$  K to describe alignment of  $\hat{\mathbf{a}}_1$  with  $\mathbf{J}$  prior to photon absorption. As we discuss below, this is actually a lower limit for  $T_0$ , which is presumably attained in

<sup>2</sup> If  $\hat{\mathbf{a}}_1$  and  $\mathbf{J}$  are not parallel and  $I_2 \neq I_3$ , the molecule nutates. Because of nutation, the rotational motion around  $\hat{\mathbf{a}}_1$  is only quasiperiodic, and the centrifugal and Coriolis stresses responsible for the IVRET process will have Fourier components over a range of frequencies around the mean rotation rate  $\omega_{\text{rot}}$  (i.e., the rotation rate averaged over the nutation period). This facilitates the coupling of rotation and vibrations via the IVRET process.

TABLE 1  
SELECTED CASES FOR A DISK MOLECULE WITH  $N_C = 200$

Parameter	case (a) CNM	case (b) Orion Bar	case (c) STR	case (d) $\hat{\mathbf{a}}_1 \parallel \mathbf{J}$
$T_{\text{rot}}$ (K)	80	220	1000	$\infty$
$T_0$ (K)	65	150	60	–
$\gamma_0$	1.2	1.5	17	$\infty$
$\gamma_r$ (3.3 $\mu\text{m}$ )	0.10	0.28	1.3	$\infty$
$\gamma_r$ (7.7 $\mu\text{m}$ )	0.27	0.73	3.3	$\infty$
$\gamma_r$ (11.3 $\mu\text{m}$ )	0.40	1.1	5.0	$\infty$
$\gamma_r$ (17 $\mu\text{m}$ )	0.67	1.5	8.3	$\infty$
$p_{\star}^{\parallel}(\pi/2)$ , 3.3 $\mu\text{m}$ (%)	0.02	0.06	1.29	7.69
$p_{\star}^{\parallel}(\pi/2)$ , 7.7 $\mu\text{m}$ (%)	0.05	0.17	3.29	7.69
$p_{\star}^{\perp}(\pi/2)$ , 11.3 $\mu\text{m}$ (%)	–0.14	–0.53	–8.56	–14.29
$p_{\star}^{\perp}(\pi/2)$ , 17 $\mu\text{m}$ (%)	–0.25	–0.73	–10.54	–14.29

cold interstellar clouds, whereas in bright photodissociation regions like the Orion Bar the radiation field is so dense that PAH grains stay always hotter.

As anticipated in §2.4, we assume that the grain disalignment between principal axis  $\hat{\mathbf{a}}_1$  and angular momentum  $\mathbf{J}$  may be described by the probability distribution in eq. (17) with “internal alignment” coefficient  $\gamma_0$  just before UV absorption, and  $\gamma_r$  during IR emission. The ratio  $T_{\text{rot}}/T_{\text{ia}}$  depends on environmental conditions, hence so does  $\gamma$  in eq. (18). We now discuss four possible cases, summarized in Table 1; for each case, we compute the value of  $\gamma_0$  prior to absorption of starlight photons, and the values of  $\gamma_r$  during emission of radiation in the 3.3, 7.7, 11.3 and 17  $\mu\text{m}$  bands.

#### 2.5.1. Case (a): CNM

In H I clouds with gas kinetic temperature  $T_{\text{gas}} \approx 100$  K (the “Cold Neutral Medium”, or CNM), the rotational excitation model by Draine & Lazarian (1998) predicts that a PAH with  $N_C = 200$  should be spinning with rotational temperature  $T_{\text{rot}} \approx 80$  K, which corresponds to a rotation frequency  $\omega_{\text{rot}}/2\pi \approx 10$  GHz. Since the molecule’s angular momentum stays approximately constant between UV absorption and IR emission, we may assume  $T_{\text{rot}} \approx 80$  K during the whole process. If  $T_0 \approx 65$  K prior to UV absorption, as discussed above, the internal alignment coefficient of our model PAH will be  $\gamma_0 \approx 1.2$ ; the values of  $\gamma_r$  for different IR emission bands are listed in Table 1.

We note that, if gas collisions were frequent enough to drive the emitting grains towards “Brownian rotation” between two subsequent UV absorptions, then the probability distribution in eq. (19) should be used instead of eq. (17) to describe the internal alignment prior to UV absorption, whereas eq. (17) may still be used during IR emission with an appropriate choice for  $\gamma_r$ . However, as discussed in the Appendix, identical polarization results may be obtained in the current formalism if we employ an “effective” internal alignment coefficient  $\gamma_0 \approx 1.0$  before UV absorption, similar to the value  $\gamma_0 = 1.2$  adopted for case (a).

#### 2.5.2. Case (b): The Orion Bar PDR

The Orion Bar, illuminated by the Trapezium stars, is an example of a bright photodissociation region (PDR), with strong PAH emission at 3.3  $\mu\text{m}$  (Tielens et al. 1993). Physical conditions in the photodissociation zone have

been discussed by Allers et al. (2005), who estimate  $n_{\text{H}} \approx 7 \times 10^4 \text{ cm}^{-3}$ ,  $T_{\text{gas}} \approx 1000$  K, and  $\chi \approx 3 \times 10^4$ , where  $n_{\text{H}}$  is the hydrogen number density and  $\chi$  is the specific radiation energy density at 1000 Å relative to the value in the local interstellar radiation field. For these conditions, the rotational excitation model of Draine & Lazarian (1998) yields a rotational temperature  $T_{\text{rot}} \approx 220$  K for a PAH with  $N_C = 200$ .

In the intense radiation field of a bright PDR, the vibrational energy of our model PAH is always large enough (and the vibrational levels sufficiently closely spaced) that the internal alignment temperature  $T_{\text{ia}}$  roughly equals the instantaneous vibrational temperature  $T_{\text{vib}}$  at any time. For a PAH molecule with  $N_C = 200$  in a radiation field with  $\chi \approx 3 \times 10^4$ , the lattice can hardly cool below  $T_{\text{vib}} \approx 150$  K (Draine & Li 2001), so that in a PDR like the Orion Bar  $T_0 \approx 150$  K may be appropriate prior to UV absorption. The corresponding internal alignment coefficient will be  $\gamma_0 \approx 1.5$  for  $T_{\text{rot}} \approx 220$  K. Values of  $\gamma_r$  for different emission bands are given in Table 1; since  $T_{\text{vib}}$  never drops below  $\approx 150$  K, we take  $T_{\text{ia}} \approx 150$  K as the characteristic internal alignment temperature for emission in the 17  $\mu\text{m}$  band.

#### 2.5.3. Case (c): Suprathermal Rotation (STR)

As discussed in §2.5.1 and 2.5.2, PAH molecules in the CNM should have moderately sub-thermal rotation rates ( $T_{\text{rot}} \lesssim T_{\text{gas}}$ ), whereas  $T_{\text{rot}} \ll T_{\text{gas}}$  in bright PDRs like the Orion Bar. Observations of microwave emission from spinning grains in the diffuse ISM (e.g., Dobler & Finkbeiner 2008; Dobler et al. 2008) and in PDRs (e.g., Casassus et al. 2008) appear to be consistent with these estimates.

However, it is of interest to explore the possibility that some PAHs might be subject to systematic torques which could spin them up to higher rotation rates. For example, inelastic collisions between a grain and hydrogen atoms may be followed by ejection of  $\text{H}_2$  molecules when a C-H bond is broken through photo- or thermo-dissociation triggered by the absorption of UV photons. If recombination of H atoms preferentially occurs at a few catalytic centers spread over the grain surface, and the  $\text{H}_2$  ejection is systematically asymmetric, the resulting torque may significantly spin up the PAH molecule.

For case (c) we assume  $T_{\text{rot}} \sim 10 T_{\text{gas}} \approx 1000$  K for PAHs in H I clouds, corresponding to a rotation frequency  $\omega_{\text{rot}}/2\pi \approx 30$  GHz for our model grain with  $N_C = 200$  carbon atoms. For PAHs spinning at 30 GHz, efficient energy transfer between vibrations and rotation via the IVRET process is suppressed, due to insufficient density of vibrational states, when the lattice cools below  $T_{\text{vib}} \approx 60$  K, hence we take  $T_0 \approx 60$  K as the internal alignment temperature prior to UV absorption, giving an internal alignment coefficient  $\gamma_0 \approx 17$ . Values of  $\gamma_r$  for different PAH emission bands are listed in Table 1.

#### 2.5.4. Case (d): $\hat{\mathbf{a}}_1 \parallel \mathbf{J}$

The physics of internal relaxation in cold, spinning grains is not well understood, and perhaps there is a slow process that couples the rotational degrees of freedom to the lattice down to very low temperatures, regardless of the lower limit imposed by the density of vibrational states. Since in H I clouds the interval between two subsequent photon absorptions is long ( $\sim 10^7$  s), there is a

lot of time for a weak process to act. Such a process would lead to  $\gamma_0 \gg 1$ , and we discuss  $\gamma_0 = \infty$  as a limiting case.

Also, if the coupling between rotation and vibrations after UV absorption took place on timescales much longer than the duration of the IR emission burst ( $\sim 1 - 10$  s), the internal alignment temperature during IR emission would stay roughly equal to the value before UV absorption. If  $\gamma_0 \gg 1$ , this would imply  $\gamma_r \gg 1$  as well. We therefore consider  $\gamma_0 = \infty$  and  $\gamma_r = \infty$  as the limiting case in which  $\hat{\mathbf{a}}_1$  is perfectly aligned with  $\mathbf{J}$  both before UV absorption and during IR emission.

### 3. POLARIZATION FROM PAHs ILLUMINATED BY A STAR OR A DISK GALAXY

We now compute the degree of polarization expected for in-plane and out-of-plane vibrational modes of PAH molecules when anisotropically illuminated by a star or a disk galaxy. We assume, for the sake of simplicity, that the angular momentum of emitting grains is randomly oriented in space, although it may be partially aligned by the interstellar magnetic field. Also, we suppose that the illuminating disk galaxy has a uniform surface-brightness profile. However, the formalism developed in §2 can be applied without such restrictions, and we discuss below how to relax these two assumptions. The grain alignment between  $\hat{\mathbf{a}}_1$  and  $\mathbf{J}$  is described via the probability distribution in eq. (17) both before UV absorption ( $dP_{\gamma_0}$ ) and during IR emission ( $dP_{\gamma_r}$ ), with “internal alignment” coefficients  $\gamma_0$  and  $\gamma_r$  respectively.

For a population of PAH molecules illuminated by a point source, the emission polarized along a direction  $\hat{\mathbf{w}}$  (= either  $\hat{\mathbf{u}}$  or  $\hat{\mathbf{v}}$  – see Fig. 1 *a*) for in-plane ( $\parallel$ ) and out-of-plane ( $\perp$ ) modes is

$$I_{\star, w}^{\parallel, \perp}(\alpha, \gamma_0, \gamma_r) \propto \int_{-1}^1 d \cos \theta \int_0^{2\pi} d\varphi \int_0^\pi dP_{\gamma_0}(\beta_0) \int_0^\pi dP_{\gamma_r}(\beta_r) \times \bar{A}_\star(\theta, \beta_0) \bar{F}_w^{\parallel, \perp}(\theta, \varphi, \beta_r, \alpha), \quad (20)$$

where  $\bar{A}_\star$  and  $\bar{F}_w^{\parallel, \perp}$  are the absorption and emission cross sections computed in §2.2 and §2.3 respectively. If the grain angular momentum is not isotropically oriented in space, it is easy to incorporate the corresponding  $(\theta, \varphi)$ -distribution function into the above integral. The polarized emission from PAHs above the center of a uniform-brightness disk galaxy is

$$I_{\text{gal}, w}^{\parallel, \perp}(\alpha, \gamma_0, \gamma_r, \omega) \propto \int_{-1}^1 d \cos \theta \int_0^{2\pi} d\varphi \int_0^\pi dP_{\gamma_0}(\beta_0) \int_0^\pi dP_{\gamma_r}(\beta_r) \times \int_{\cos \omega}^1 \frac{d \cos \theta'}{\Omega} \bar{A}_{\text{gal}}(\theta, \beta_0, \theta') \bar{F}_w^{\parallel, \perp}(\theta, \varphi, \beta_r, \alpha), \quad (21)$$

where  $\Omega = 2\pi(1 - \cos \omega)$  is the solid angle subtended by the galactic disk as seen from the emitting molecules. A generic axisymmetric surface-brightness profile  $B(\theta')$  can be easily included in the previous expression.

The resulting degree of polarization for in-plane and out-of-plane modes is respectively

$$p^{\parallel, \perp} \equiv \frac{I_u^{\parallel, \perp} - I_v^{\parallel, \perp}}{I_u^{\parallel, \perp} + I_v^{\parallel, \perp}}, \quad (22)$$

and will therefore be positive for emission polarized along  $\hat{\mathbf{u}}$  and negative for polarization along  $\hat{\mathbf{v}}$ .

#### 3.1. Polarization from PAHs illuminated by a star

By integrating eq. (20), we obtain the degree of polarization for in-plane and out-of-plane modes from a population of PAH molecules illuminated by a star (or a generic point source)

$$p_\star^\parallel(\alpha, \gamma_0, \gamma_r) = \frac{3 \sin^2 \alpha}{640 h(\gamma_0)h(\gamma_r) + 3 \cos^2 \alpha - 1}, \quad (23)$$

$$p_\star^\perp(\alpha, \gamma_0, \gamma_r) = \frac{-3 \sin^2 \alpha}{320 h(\gamma_0)h(\gamma_r) - 3 \cos^2 \alpha + 1}, \quad (24)$$

where  $\alpha$  is the angle between the line of sight and the illumination direction (see Fig. 1 *a*), and

$$\begin{aligned} g_1(\gamma) &\equiv \sqrt{\pi} \gamma \operatorname{erfi}(\sqrt{\gamma}) \quad , \\ g_2(\gamma) &\equiv 6 \sqrt{\gamma} e^\gamma - (3 + 2\gamma)\sqrt{\pi} \operatorname{erfi}(\sqrt{\gamma}) \quad , \\ h(\gamma) &\equiv g_1(\gamma)/g_2(\gamma) \quad . \end{aligned} \quad (25)$$

The function  $h(\gamma)$  monotonically decreases from  $h(0) \rightarrow \infty$  to  $h(\gamma \rightarrow \infty) = 1/4$ . Since  $h(0) \rightarrow \infty$ , if the grain principal axis of inertia is randomly oriented with respect to the angular momentum either before or after UV absorption, the emitted radiation is completely unpolarized. Since  $h(\gamma) > 1/4$ , we have  $p_\star^\parallel \geq 0$  and  $p_\star^\perp \leq 0$  for any choice of  $\gamma_0, \gamma_r$  and  $\alpha$ . According to the definition in eq. (22), this means that in-plane and out-of-plane modes are polarized respectively along  $\hat{\mathbf{u}}$  and along  $\hat{\mathbf{v}}$ , confirming Leger’s (1988) prediction that the polarization direction for in-plane and out-of-plane modes is respectively orthogonal and parallel to the plane-of-sky projection of the illumination direction (see Fig. 1 *a*).

For fixed  $\gamma_0$  and  $\gamma_r$ , eqs. (23) and (24) show that the IR emission bands should be maximally polarized when  $\alpha = \pi/2$ , i.e., the line of sight to the emitting PAHs is orthogonal to the star-molecule direction. For this optimal viewing geometry, Table 1 reports the degree of polarization expected for the 3.3, 7.7, 11.3 and 17  $\mu\text{m}$  emission features in different environmental conditions, as discussed in §2.5; we have assumed the 17  $\mu\text{m}$  band to arise from out-of-plane modes. Figure 2 shows the dependence of  $p_\star^\parallel(\pi/2)$  and  $p_\star^\perp(\pi/2)$  on the internal alignment coefficient  $\gamma_0$ , with the different curves corresponding to different values of the ratio  $\gamma_r/\gamma_0$ . Because  $\gamma_r \leq \gamma_0$ , the region to the left of the solid lines is excluded. In most cases, the dependence on the viewing angle  $\alpha$  in the denominator of eqs. (23)-(24) can be neglected, hence  $p_\star^\parallel(\alpha, \gamma_0, \gamma_r) \approx p_\star^\parallel(\pi/2, \gamma_0, \gamma_r) \sin^2 \alpha$ , and similarly for  $p_\star^\perp$  (compare solid and dotted lines in Fig. 3).

For the extreme case of perfect alignment between  $\hat{\mathbf{a}}_1$  and  $\mathbf{J}$  during both UV absorption ( $\gamma_0 = \infty$ ) and IR emission ( $\gamma_r = \infty$ ), corresponding to case (d) in §2.5, eqs. (23) and (24) may be simplified:

$$p_\star^\parallel(\alpha) = \frac{\sin^2 \alpha}{13 + \cos^2 \alpha}, \quad (26)$$

$$p_\star^\perp(\alpha) = \frac{-\sin^2 \alpha}{7 - \cos^2 \alpha}. \quad (27)$$

#### 3.2. Polarization from PAHs illuminated by a uniform-brightness disk galaxy

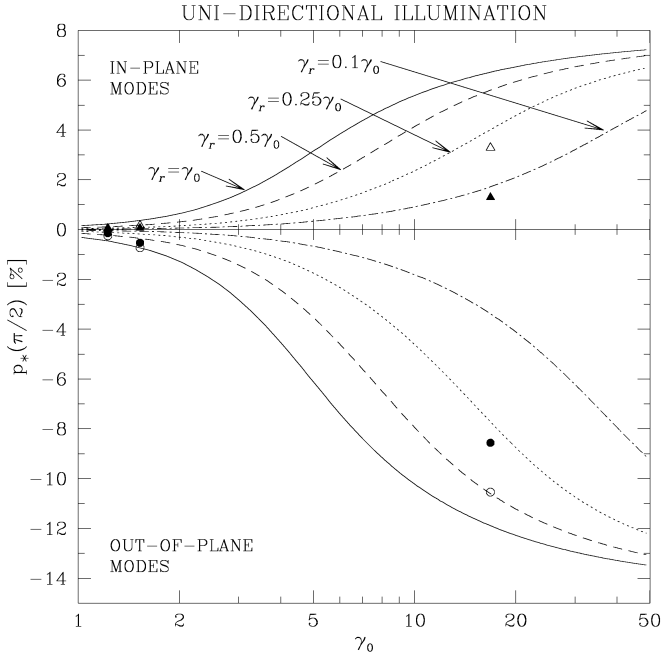


FIG. 2.— For PAHs illuminated by a star, dependence of the polarization  $p_*$  on  $\gamma_0$ , for optimal viewing geometry ( $\alpha = \pi/2$ ). The different lines correspond to different values of the ratio  $\gamma_r/\gamma_0$ :  $\gamma_r = \gamma_0$  (solid),  $\gamma_r = 0.5\gamma_0$  (dashed),  $\gamma_r = 0.25\gamma_0$  (dotted), and  $\gamma_r = 0.1\gamma_0$  (dot-dashed). The polarization values reported in Table 1 are shown as solid triangles ( $3.3\ \mu\text{m}$ ), open triangles ( $7.7\ \mu\text{m}$ ), solid circles ( $11.3\ \mu\text{m}$ ), and open circles ( $17\ \mu\text{m}$ , assumed to arise from out-of-plane modes), with different values of  $\gamma_0$  corresponding to case (a) ( $\gamma_0 = 1.2$ ), case (b) ( $\gamma_0 = 1.5$ ) or case (c) ( $\gamma_0 = 17$ ).

The degree of polarization for in-plane and out-of-plane modes from a population of PAH molecules above the center of a uniform-brightness disk galaxy is obtained from eq. (21):

$$p_{\text{gal}}^{\parallel}(\alpha, \gamma_0, \gamma_r, \omega) = \frac{3 \sin^2 \alpha}{1280 \frac{h(\gamma_0)h(\gamma_r)}{(\cos^2 \omega + \cos \omega)} + 3 \cos^2 \alpha - 1}, \quad (28)$$

$$p_{\text{gal}}^{\perp}(\alpha, \gamma_0, \gamma_r, \omega) = \frac{-3 \sin^2 \alpha}{640 \frac{h(\gamma_0)h(\gamma_r)}{(\cos^2 \omega + \cos \omega)} - 3 \cos^2 \alpha + 1}, \quad (29)$$

where  $\Omega = 2\pi(1 - \cos \omega)$  is the angle subtended by the galaxy as seen from the emitting grains. The limit  $\Omega \rightarrow 0$  recovers the case of a point-like illuminating source in eqs. (23) and (24), whereas for an infinite disk ( $\Omega \rightarrow 2\pi$ ) the degree of polarization tends to zero. Figure 4 shows, for the most favorable viewing geometry ( $\alpha = \pi/2$ ), the dependence of the degree of polarization on  $\gamma_0$  for PAHs illuminated by a disk galaxy with  $\Omega = \pi$ ; the different curves correspond to different values of  $\gamma_0/\gamma_r$ , as explained in §3.1. For diffuse illumination with  $\Omega = \pi$ , we find levels of polarization that are  $\sim 40\%$  of the values found for uni-directional illumination.

The extreme case of grains with perfect internal alignment ( $\hat{\mathbf{a}}_1 \parallel \mathbf{J}$  during both UV absorption and IR emission, case (d) in §2.5) yields

$$p_{\text{gal}}^{\parallel}(\alpha, \omega) = \frac{3 \sin^2 \alpha}{80(\cos^2 \omega + \cos \omega)^{-1} + 3 \cos^2 \alpha - 1}, \quad (30)$$

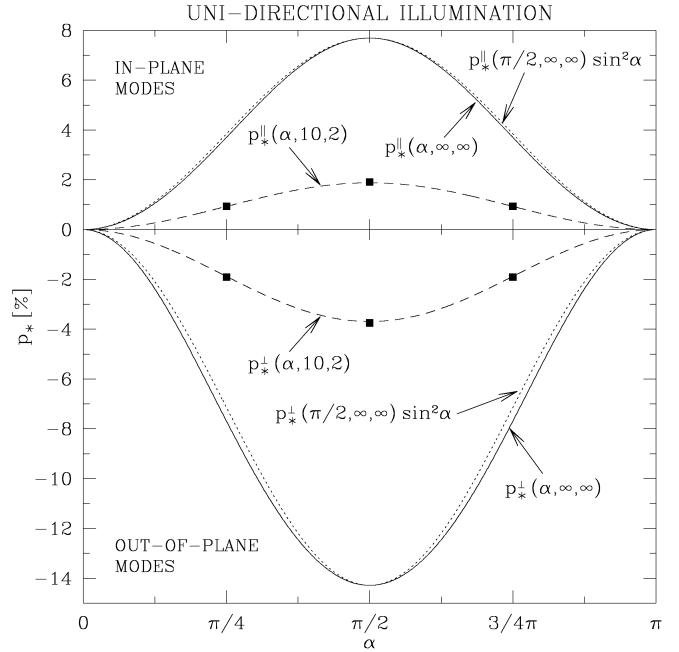


FIG. 3.— For PAHs illuminated by a star, dependence of the polarization  $p_*(\alpha, \gamma_0, \gamma_r)$  on the viewing angle  $\alpha$ . Dashed line: polarization for  $(\gamma_0, \gamma_r) = (10, 2)$ , similar to case (c) in §2.5. The polarization values quoted by Leger (1988) for a disk molecule are shown as solid squares, and are seen to match the values calculated for  $(\gamma_0, \gamma_r) = (10, 2)$ . Solid line: polarization for perfect internal alignment  $(\gamma_0, \gamma_r) = (\infty, \infty)$  (see eqs. (26)-(27)), corresponding to case (d) in §2.5. The dotted line is  $p_*^{\perp}(\pi/2) \sin^2 \alpha$  for  $(\gamma_0, \gamma_r) = (\infty, \infty)$ , which closely approximates the dependence on  $\alpha$  of eqs. (26)-(27).

$$p_{\text{gal}}^{\perp}(\alpha, \omega) = \frac{-3 \sin^2 \alpha}{40(\cos^2 \omega + \cos \omega)^{-1} - 3 \cos^2 \alpha + 1}. \quad (31)$$

#### 4. DISCUSSION AND SUMMARY

We have obtained analytic formulae for the degree of polarization expected for the 3.3, 6.2, 7.7, 8.6, 11.3, 12.7, 16.4, and  $17\ \mu\text{m}$  emission features when the emitting PAHs are anisotropically illuminated by a source of UV photons. We model PAH grains as planar molecules with in-plane and out-of-plane vibrational dipoles. Vibrational modes oscillating in the molecular plane (responsible for the 3.3, 6.2, 7.7, and  $8.6\ \mu\text{m}$  emission bands) are polarized perpendicular to the plane-of-sky projection of the illumination direction, whereas for out-of-plane modes (responsible for the 11.3 and  $12.7\ \mu\text{m}$  features) the polarization is along the source-molecule direction, as originally pointed out by Leger (1988). The fact that the predicted polarization directions for in-plane and out-of-plane modes are orthogonal provides a check on the contribution to the polarization from linear dichroism by aligned foreground dust, as this would be expected to produce polarization in a single plane. It also means that polarization measurements could be used to diagnose the character (in-plane or out-of-plane) of the modes responsible for the poorly-characterized 16.4 and  $17\ \mu\text{m}$  emission features.

Our analytic formulae show explicitly how the degree of polarization depends on the viewing geometry (i.e., the angle  $\alpha$  between the line of sight and the illumina-

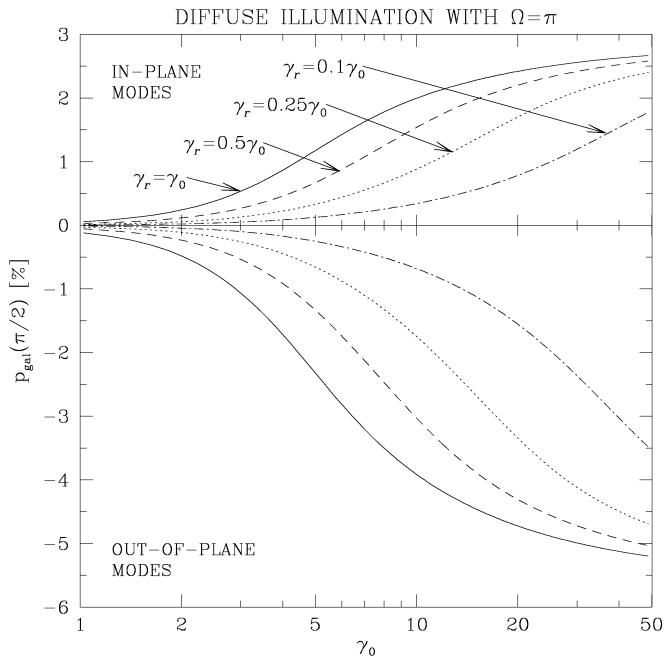


FIG. 4.— For PAHs illuminated by a disk galaxy with  $\Omega = \pi$ , dependence of the polarization  $p_{\text{gal}}$  on  $\gamma_0$ , for optimal viewing geometry ( $\alpha = \pi/2$ ). The different lines correspond to different values of the ratio  $\gamma_r/\gamma_0$ , as explained in the caption of Fig. 2.

tion direction) and the “internal alignment” coefficients  $\gamma_0$ , describing the alignment between the grain principal axis  $\hat{\mathbf{a}}_1$  and angular momentum  $\mathbf{J}$  just before UV absorption, and  $\gamma_r$ , characterizing the internal alignment during the brief period of IR emission following UV excitation. The degree of polarization is maximal for  $\alpha = \pi/2$  and, at fixed  $\alpha$ , it increases with  $\gamma_0$  and  $\gamma_r$ , as the principal axis and angular momentum become more closely aligned. We have discussed both the case of a point-like illuminating source, which may be applied to reflection nebulae and PDRs such as the Orion Bar, and of an extended source (e.g., dust above a disk galaxy like NGC 891 or M82). The degree of polarization for uni-directional illumination is higher than for diffuse illumination, all else being equal; however, if the galaxy’s surface-brightness profile is strongly peaked at the galactic center, the galaxy would resemble a point source, with polarization levels comparable to the case of uni-directional illumination.

The value of  $\gamma_r$  is expected to increase with increasing wavelength of the emission feature, since such a band will be mostly emitted when the grain is cooler and  $\hat{\mathbf{a}}_1$  and  $\mathbf{J}$  are expected to be more closely aligned. Therefore, when comparing two IR emission features arising from modes of the same character (either in-plane or out-of-plane), the band with longer wavelength should be more strongly polarized. Table 1 reports, in case of uni-directional illumination and optimal viewing geometry ( $\alpha = \pi/2$ ), the predicted degree of polarization for the 3.3, 7.7, 11.3, and 17  $\mu\text{m}$  emission features, for four exemplary choices of environmental conditions.<sup>3</sup>

<sup>3</sup> The polarization results in Table 1 assume that the PAH angular momenta are randomly oriented in space; if the grains are partially oriented, e.g., by the interstellar magnetic field, we would

expect a higher degree of polarization.

For dust in the CNM, significant disalignment between  $\hat{\mathbf{a}}_1$  and  $\mathbf{J}$  ( $\gamma_0 \approx 1$ ,  $\gamma_r \lesssim 0.5\gamma_0$ ) is expected to strongly suppress the intrinsic polarization of the IR bands, with the 3.3  $\mu\text{m}$  emission feature predicted to be polarized by only  $\approx 0.02\%$  (for our estimated  $\gamma_0 = 1.2$  and  $\gamma_r = 0.10$ ), presumably too small to distinguish from polarization due to foreground linear dichroism. Longer wavelength features are expected to be more strongly polarized (e.g.,  $-0.14\%$  for the 11.3  $\mu\text{m}$  feature, with  $\gamma_r = 0.40$ ), but the polarization levels are still observationally challenging. These conditions may apply to PAHs above the disk of an edge-on galaxy, such as NGC 891 or M82; however, the polarization degrees quoted above are computed for the case of uni-directional illumination, which is realized only if the galaxy’s luminosity is strongly concentrated at its center. If the galaxy appears to the emitting grains as an extended source, the PAH polarization will be even smaller.

The Orion Bar PDR is expected to be somewhat more favorable for the PAH internal alignment because of higher molecular rotation rates, but even there the polarization of the 3.3  $\mu\text{m}$  feature is predicted to be only  $\approx 0.06\%$  for our estimated  $(\gamma_0, \gamma_r) = (1.5, 0.28)$ . If the polarization  $0.86 \pm 0.28\%$  measured by Sellgren et al. (1988) for the 3.3  $\mu\text{m}$  emission feature is correct, it implies that we underestimated the internal alignment of emitting PAHs both before UV absorption ( $\gamma_0$ ) and during IR emission ( $\gamma_r$ ). A polarization of 0.86% for optimal viewing angle  $\alpha = \pi/2$  would require, e.g.,  $(\gamma_0, \gamma_r) = (2.3, 2.3)$ ,  $(3.0, 1.8)$ ,  $(\infty, 0.81)$ , etc.: all solutions must have  $\gamma_r \leq \gamma_0$ , hence  $\gamma_0 \geq 2.3$  and  $\gamma_r \geq 0.81$ . Such good internal alignment is not expected unless the smallest PAHs are rotating suprathermally. The polarization at 11.3  $\mu\text{m}$  is predicted to be considerably larger than the polarization at 3.3  $\mu\text{m}$  (see Table 1). Additional polarization measurements of the Orion Bar at 3.3 and 11.3  $\mu\text{m}$  are needed. If the large intrinsic polarization detected by Sellgren et al. (1988) at 3.3  $\mu\text{m}$  is confirmed, it will call into question current thinking with regard to the rotational dynamics of PAHs in PDRs, since it seems to require at least moderately suprathermal rotation rates.

Comparison of our analytic results with polarization measurements may provide useful constraints on the geometrical and dynamical properties of PAH molecules, concerning in particular: *i*) their planarity, which has been assumed *a priori* in this work, although it is still uncertain, especially for larger PAHs; *ii*) the efficacy of internal relaxation processes that can exchange energy between vibrational and rotational modes; *iii*) the possibility of systematic torques that may spin the grains up to suprathermal rotation; and *iv*) a determination, via the polarization direction, of the character of the vibrational modes contributing to a given IR feature, which will be of particular interest for the poorly-characterized 16.4 and 17  $\mu\text{m}$  bands.

If the polarization is too small to be detected, the interpretation will not be clear: it could be the result of PAH non-planarity, or a mixture of in-plane and out-of-plane contributions to the mode (this may be an issue for the 16.4 and 17  $\mu\text{m}$  features), or (more likely) it could simply derive from poor alignment of the grain principal axis  $\hat{\mathbf{a}}_1$  and angular momentum  $\mathbf{J}$ . However, if a high degree of

expect a higher degree of polarization.



polarization is observed, it will imply both that PAHs are planar *and* that their principal axis is well aligned with the angular momentum. This would be valuable information concerning the nature of PAHs and their rotational dynamics.

BTD thanks Chris Packham and Charles Telesco for helpful discussions on the possibility of polarization of the PAH features. We are grateful to R.H. Lupton for the availability of the SM graphics program. This research was supported in part by NSF grant AST-0406883.

## REFERENCES

- Allamandola, L. J., Tielens, A. G. G. M., & Barker, J. R. 1985, *ApJ*, 290, L25
- Allers, K. N., Jaffe, D. T., Lacy, J. H., Draine, B. T., & Richter, M. J. 2005, *ApJ*, 630, 368
- Casassus, S., Dickinson, C., Cleary, K., Paladini, R., Etxaluze, M., Lim, T., White, G. J., Burton, M., Indermuehle, B., Stahl, O., & Roche, P. 2008, *MNRAS*, 391, 1075
- Dobler, G., Draine, B. T., & Finkbeiner, D. P. 2008, *astro-ph/0811.1040*
- Dobler, G. & Finkbeiner, D. P. 2008, *ApJ*, 680, 1222
- Draine, B. T. & Lazarian, A. 1998, *ApJ*, 508, 157
- Draine, B. T. & Li, A. 2001, *ApJ*, 551, 807
- . 2007, *ApJ*, 657, 810
- Lazarian, A. & Draine, B. T. 1997, *ApJ*, 487, 248
- Leger, A. 1988, in *Polarized Radiation of Circumstellar Origin*, ed. G. V. Coyne, A. F. J. Moffat, S. Tapia, A. M. Magalhaes, R. E. Schulte-Ladbeck & N. C. Wickramasinghe (Vatican Observatory), 769-795
- Leger, A. & Puget, J. L. 1984, *A&A*, 137, L5
- Purcell, E. M. 1979, *ApJ*, 231, 404
- Rouan, D., Leger, A., Omont, A., & Giard, M. 1992, *A&A*, 253, 498
- Sellgren, K., Rouan, D., & Leger, A. 1988, *A&A*, 196, 252
- Smith, J. D. T., Draine, B. T., Dale, D. A., Moustakas, J., Kennicutt, R. C., Helou, G., Armus, L., Roussel, H., Sheth, K., Bendo, G. J., Buckalew, B., Calzetti, D., Engelbracht, C. W., Gordon, K. D., Hollenbach, D. J., Li, A., Malhotra, S., Murphy, E. J., & Walter, F. 2007, *ApJ*, 656, 770
- Tielens, A. G. G. M., Meixner, M. M., van der Werf, P. P., Bregman, J., Tauber, J. A., Stutzki, J., & Rank, D. 1993, *Science*, 262, 86

## APPENDIX

## POLARIZATION FROM PAHS IN BROWNIAN ROTATION

We have assumed above that the internal alignment between the principal axis  $\hat{\mathbf{a}}_1$  and angular momentum  $\mathbf{J}$  of emitting PAHs can be parametrized via the probability distribution in eq. (17) both before UV absorption (with  $\gamma_0$ ) and during IR emission (with  $\gamma_r \leq \gamma_0$ ). However, if the interval between two subsequent photon absorptions is longer than the time required for the PAH molecule to collide with its own mass of gas, and if the IVRET process is ineffective at exchanging energy between the grain rotation and the (generally colder) vibrational modes, the molecule will be driven towards “Brownian rotation” with internal alignment temperature  $T_0 \approx T_{\text{gas}}$  prior to UV absorption. In this case, the probability distribution  $dP_\epsilon$  in eq. (19) should be used instead of eq. (17) to describe the grain internal alignment before UV absorption, whereas  $dP_{\gamma_r}$  in eq. (17) with internal alignment coefficient  $\gamma_r$  may still be appropriate during IR emission. If the molecule angular momentum is randomly oriented in space, the polarized emission along a direction  $\hat{\mathbf{w}}$  (= either  $\hat{\mathbf{u}}$  or  $\hat{\mathbf{v}}$  – see Fig. 1 *a*) for in-plane and out-of-plane modes from a population of PAHs illuminated by a point-like source is

$$I_{\star,w}^{\parallel,\perp}(\alpha, \epsilon, \gamma_r) \propto \int_{-1}^1 d \cos \theta \int_0^{2\pi} d\varphi \int_0^\pi dP_\epsilon(\beta_0) \int_0^\pi dP_{\gamma_r}(\beta_r) \bar{A}_\star(\theta, \beta_0) \bar{F}_w^{\parallel,\perp}(\theta, \varphi, \beta_r, \alpha) \quad . \quad (\text{A1})$$

The corresponding expression for PAH molecules above the center of a uniform-brightness disk galaxy is

$$I_{\text{gal},w}^{\parallel,\perp}(\alpha, \epsilon, \gamma_r, \omega) \propto \int_{-1}^1 d \cos \theta \int_0^{2\pi} d\varphi \int_0^\pi dP_\epsilon(\beta_0) \int_0^\pi dP_{\gamma_r}(\beta_r) \int_{\cos \omega}^1 \frac{d \cos \theta'}{\Omega} \bar{A}_{\text{gal}}(\theta, \beta_0, \theta') \bar{F}_w^{\parallel,\perp}(\theta, \varphi, \beta_r, \alpha) \quad , \quad (\text{A2})$$

where  $\Omega = 2\pi(1 - \cos \omega)$  is the solid angle subtended by the galactic disk as seen from the emitting molecules. The degree of polarization can then be computed from eq. (22). Let us define

$$q(\epsilon) \equiv 3 \epsilon [1 - \sqrt{\epsilon - 1} \arcsin(1/\sqrt{\epsilon})] - 1 \quad , \quad (\text{A3})$$

where  $\epsilon \equiv I_1/(I_1 - I_2)$ . Making use of  $h(\gamma)$  as defined in eq. (25), the polarization for in-plane and out-of-plane modes in case of uni-directional illumination is

$$p_\star^\parallel(\alpha, \epsilon, \gamma_r) = \frac{3 \sin^2 \alpha}{320 h(\gamma_r)/q(\epsilon) + 3 \cos^2 \alpha - 1} \quad , \quad (\text{A4})$$

$$p_\star^\perp(\alpha, \epsilon, \gamma_r) = \frac{-3 \sin^2 \alpha}{160 h(\gamma_r)/q(\epsilon) - 3 \cos^2 \alpha + 1} \quad , \quad (\text{A5})$$

whereas for diffuse illumination by a uniform-brightness disk galaxy we have

$$p_{\text{gal}}^\parallel(\alpha, \epsilon, \gamma_r, \omega) = \frac{3 \sin^2 \alpha}{640 \frac{h(\gamma_r)/q(\epsilon)}{(\cos^2 \omega + \cos \omega)} + 3 \cos^2 \alpha - 1} \quad , \quad (\text{A6})$$

$$p_{\text{gal}}^\perp(\alpha, \epsilon, \gamma_r, \omega) = \frac{-3 \sin^2 \alpha}{320 \frac{h(\gamma_r)/q(\epsilon)}{(\cos^2 \omega + \cos \omega)} - 3 \cos^2 \alpha + 1} \quad . \quad (\text{A7})$$

Comparison of these formulae with eqs. (23)-(24) and eqs. (28)-(29) shows that the polarization results obtained here can be exactly reproduced by the probability distribution in eq. (17) if we adopt an “effective” internal alignment coefficient  $\gamma_0$  before UV absorption satisfying  $2 h(\gamma_0) = 1/q(\epsilon)$ . For  $\epsilon = 2$ , as appropriate for our model PAH with  $I_1/I_2 = 2$ , the solution is  $\gamma_0 \approx 1.0$ .